letters to nature

While several other mechanisms (for example, perturbations in a binary star[18], resonances[10], interaction with a gaseous disk[11]) have been proposed to explain the large eccentricities of extrasolar planets, only planet–planet scattering naturally results in an impulsive perturbation—which is necessary to explain the υ And system. All other mechanisms operate on much longer timescales and would also affect the eccentricity of υ And c, erasing the memory of its initial circular orbit (see Supplementary Information for a more detailed discussion).

Our results have other implications for planet formation. Given the difficulty of forming giant planets at small orbital distances, it is generally assumed that the υ And planets migrated inward to their current locations via interactions with the protoplanetary disk[12]. If this is correct, then the small minimum eccentricity of υ And c also provides evidence that its eccentricity at the end of migration had not grown significantly, in contrast to what some theories predict[11]. However, the possibility of formation *in situ*[19] cannot be excluded by our results. ☐

1. Schneider, J. *Extra-solar Planets Catalog* (http://cfa-www.harvard.edu/planets/catalog.html) (2005).
2. Butler, R. P. *et al.* Evidence for multiple companions to Upsilon Andromedae. *Astrophys. J.* **526**, 916–927 (1999).
3. Fischer, D. A. *et al.* A planetary companion to HD 40979 and additional planets orbiting HD 12661 and HD 38529. *Astrophys. J.* **586**, 1394–1408 (2003).
4. Malhotra, R. A dynamical mechanism for establishing apsidal resonance. *Astrophys. J. Lett.* **575**, L33–L36 (2002).
5. Rasio, F. A., Tout, C. A., Lubow, S. H. & Livio, M. Tidal decay of close planetary orbits. *Astrophys. J.* **470**, 1187–1191 (1996).
6. Stepinski, T. F., Malhotra, R. & Black, D. C. The Upsilon Andromedae system: models and stability. *Astrophys. J.* **545**, 1044–1057 (2000).
7. Chiang, E. I., Tabachnik, S. & Tremaine, S. Apsidal alignment in Upsilon Andromedae. *Astron. J.* **122**, 1607–1615 (2001).
8. Rasio, F. A. & Ford, E. B. Dynamical instabilities and the formation of extrasolar planetary systems. *Science* **274**, 954–956 (1996).
9. Weidenschilling, S. J. & Marzari, F. Gravitational scattering as a possible origin for giant planets at small stellar distances. *Nature* **384**, 619–621 (1996).
10. Chiang, E. I. & Murray, N. Eccentricity excitation and apsidal resonance capture in the planetary system Upsilon Andromedae. *Astrophys. J.* **576**, 473–477 (2002).
11. Goldreich, P. & Sari, R. Eccentricity evolution for planets in gaseous disks. *Astrophys. J.* **585**, 1024–1037 (2003).
12. Lin, D. N. C. *et al.* in *Protostars and Planets IV* (eds Mannings, V., Boss, A. P. & Russell, S. S.) 1111–1178 (Univ. Arizona Press, Tucson, 2000).
13. Lissauer, J. J. & Rivera, E. J. Stability analysis of the planetary system orbiting Upsilon Andromedae. II. Simulations using new Lick Observatory fits. *Astrophys. J.* **554**, 1141–1150 (2001).
14. Lystad, V. & Rasio, F. in *The Search for Other Worlds* (eds Holt, S. S. & Deming, D.) 273–276 (AIP Conf. Proc. 713, American Institute of Physics, New York, 2004).
15. Ford, E. B., Havlickova, M. & Rasio, F. A. Dynamical instabilities in extrasolar planetary systems containing two giant planets. *Icarus* **150**, 303–313 (2001).
16. Ford, E. B., Rasio, F. A. & Yu, K. in *Scientific Frontiers in Research on Extrasolar Planets* (eds Deming, D. & Seager, S.) 181–187 (ASP Conf. Ser. 294, Astronomical Society of the Pacific, San Francisco, 2003).
17. Marzari, E. F. & Weidenschilling, S. J. Eccentric extrasolar planets: the jumping Jupiter model. *Icarus* **156**, 570–579 (2002).
18. Holman, M., Touma, T. & Tremaine, S. Chaotic variations in the eccentricity of the planet orbiting 16 Cyg B. *Nature* **386**, 254–256 (1997).
19. Bodenheimer, P., Hubickyj, O. & Lissauer, J. J. Models of the in situ formation of detected extrasolar giant planets. *Icarus* **143**, 2–14 (2000).
20. Ford, E. B. Quantifying the uncertainty in the orbits of extrasolar planets. *Astron. J.* (in the press).
21. Chambers, J. E. A hybrid symplectic integrator that permits close encounters between massive bodies. *Mon. Not. R. Astron. Soc.* **304**, 793–799 (1999).
22. Murray, C. D. & Dermott, S. F. *Solar System Dynamics* (Cambridge Univ. Press, New York, 1999).
23. Gladman, B. Dynamics of systems of two close planets. *Icarus* **106**, 247–265 (1993).

Sensitivity gains in chemosensing by lasing action in organic polymers

Aimée Rose[1], Zhengguo Zhu[1], Conor F. Madigan[2], Timothy M. Swager[1] & Vladimir Bulović[2]

[1]*Department of Chemistry and* [2]*Department of Electrical Engineering and Computer Science, Massachusetts Institute of Technology, Cambridge, Massachusetts 02139, USA*

Societal needs for greater security require dramatic improvements in the sensitivity of chemical and biological sensors. To meet this challenge, increasing emphasis in analytical science has been directed towards materials and devices having highly non-linear characteristics; semiconducting organic polymers (SOPs), with their facile excited state (exciton) transport, are prime examples of amplifying materials[1–3]. SOPs have also been recognized as promising lasing materials[4], although the susceptibility of these materials to optical damage has thus far limited applications. Here we report that attenuated lasing in optically pumped SOP thin films displays a sensitivity to vapours of explosives more than 30 times higher than is observed from spontaneous emission. Critical to this achievement was the development of a transducing polymer with high thin-film quantum yield, a high optical damage threshold in ambient atmosphere and a record low lasing threshold. Trace vapours of the explosives 2,4,6-trinitrotoluene (TNT) and 2,4-dinitrotoluene (DNT) introduce non-radiative deactivation pathways[5] that compete with stimulated emission. We demonstrate that the induced cessation of the lasing action, and associated sensitivity enhancement, is most pronounced when films are pumped at intensities near their lasing threshold. The combined gains from amplifying materials and lasing promise to deliver sensors that can detect explosives with unparalleled sensitivity.

One of the successes for SOP-based sensors has been the ultra-trace detection of vapours of TNT and DNT using SOP thin films[5], which enables the detection of buried landmines on the basis of an explosive vapour signature[6]. The detection of TNT/DNT is facilitated by the electron-deficient-acidic nature of nitroaromatics that bind to the electron-rich semiconducting polymer and quench its fluorescence by an electron transfer mechanism. The emission quenching is enhanced when the excitons rapidly diffuse throughout the SOPs, thereby increasing the probability of an encounter with the TNT/DNT. The low vapour pressure of DNT and TNT (about 100 p.p.b. and 5 p.p.b., respectively) and their efficiency for reversible fluorescence quenching make them ideal analytes to explore novel sensitivity augmentation mechanisms in SOP sensors. Previous approaches to increasing the signal gain in these systems focused on extending the exciton diffusion length by increasing excited state lifetimes and by producing emissive three-dimensional electronic delocalization[7,8]. Here we demonstrate a different enhancement mechanism that can complement all of these other schemes by harnessing the amplifying nature of the SOP lasing action to generate greater sensitivity. We demonstrate with this new approach a more than 30-fold increase in detection sensitivity when operating near the lasing threshold.

Lasing in both SOPs[4] and molecular organic materials[9,10] can generally be obtained for materials with high photoluminescence efficiencies and large Stokes shifts (that minimize the light reabsorption losses)[11]. However, a limitation of these organic materials has been the lack of durability under the punishing conditions of high pump powers, ambient atmosphere and extended operation, all of which are necessary for many sensory applications. Polymer **1** (Fig. 1) was designed to meet these demanding photophysical and stability needs and also to be sensitive to the chosen analytes, TNT

and DNT. In thin film form, **1** displays a luminescence peak maximum at wavelength $\lambda = 500$ nm. The rapid radiative relaxation (with fluorescence lifetime of $\sim$650 ps) contributes to its high fluorescence efficiency in spin-cast thin films of $\Phi = 80\%$, measured by comparison to a standard of 9,10-diphenylanthracene in polymethylmethacrylate ($\Phi = 83\%$). A noteworthy design feature of **1** is the pendant aromatic rings that result in the attachment of hydrocarbon side chains parallel to the polymer backbone, which effectively encapsulate the polymer backbone. We suggest that this encapsulation provides a protective sheath that prevents self-quenching and may provide resistance to photobleaching. The extended π-orbital interactions in **1** create a band structure that facilitates exciton diffusion lengths of 7–15 nm (for studies of exciton diffusion lengths in related poly(phenylene-vinylene)s see ref. 12; see also ref. 13). We observe chemical sensitivity enhancements in the lasing action of **1** when it is fabricated into simple waveguides (Fig. 1a), applied over distributed feedback (DFB) gratings (Fig. 1b), or coated on the exterior of an optical fibre (Fig. 1c). The consistent lasing action sensitivity enhancement for all devices confirms a general principle that is independent of architecture.

Multimode lasing action (see Supplementary Information part D) in thin films of **1** is generated under ambient atmosphere by optically exciting structures with 4-ns nitrogen laser pulses ($\lambda = 337$ nm) at an operating frequency of 30 Hz. The excitation

laser beam was focused into a 9 mm × 0.09 mm stripe, and the emission was collected at a 60° angle from the excitation beam, which was incident normal to the substrate. In initial experiments, simple asymmetric waveguides were formed by spin-casting solutions of **1** (50 mg per ml hexane) into thin films with thicknesses ranging from 30 nm to 400 nm on glass substrates. In films thicker than 50 nm, we observe a multimode amplified spontaneous emission (ASE) which peaks at $\lambda = 535$ nm, a wavelength coinciding with the first vibronic transition (0,1) of **1**. The (0,0) transition dominates the spontaneous emission owing to its higher oscillator strength. The selective ASE from the (0,1) mode is probably governed by the reabsorption losses that inhibit ASE from the (0,0) transitions.

Earlier studies demonstrated that TNT and DNT bind tightly to electron-rich SOPs such as **1**, and with short exposures these analytes are localized to the film surface[4]. As polymer **1** exciton diffusion length normal to the surface is 7–15 nm (ref. 14), similar film thicknesses of **1** are needed to ensure that the TNT/DNT exciton quenching at the surface is not overshadowed by unattenuated bulk emission. Such thin SOP films, however, would not sustain the guided light intensities needed for initiation of ASE and lasing action. Planar waveguides were therefore formed by spin-coating a thin film of **1** (with refractive index $n = 1.7$) on a transparent, index-matched thick film of parylene (with $n = 1.67$), which guides most of the photoexcited radiation (Fig. 1a). In these structures, we observed ASE for SOP layers as thin as 40 nm, with thinner films absorbing an insufficient amount of the excitation light. Comparisons of the emission intensities of the (0,0) band at $\lambda = 500$ nm and the (0,1) band at $\lambda = 535$ nm in an 80-nm-thick film of **1** on parylene as a function of pump power reveal the onset of ASE at the integrated threshold power of 80 nW. This corresponds to a threshold peak pump power of $P_{TH} = 82$ W cm^{-2} for each pulse and a pump threshold energy of $E_{TH} = 330$ nJ cm^{-2} per pulse. At these low pumping levels, the signal attenuation due to photobleaching exposure is negligible (see Supplementary Information part C). When a 40-nm-thick film of **1** is deposited onto the DFB structures[15], the threshold energy is further reduced to $E_{TH} = 40$ nJ cm^{-2}, corresponding to a peak pump power of $P_{TH} = 10$ W cm^{-2} (Fig. 2), further lowering the associated photo-oxidation.
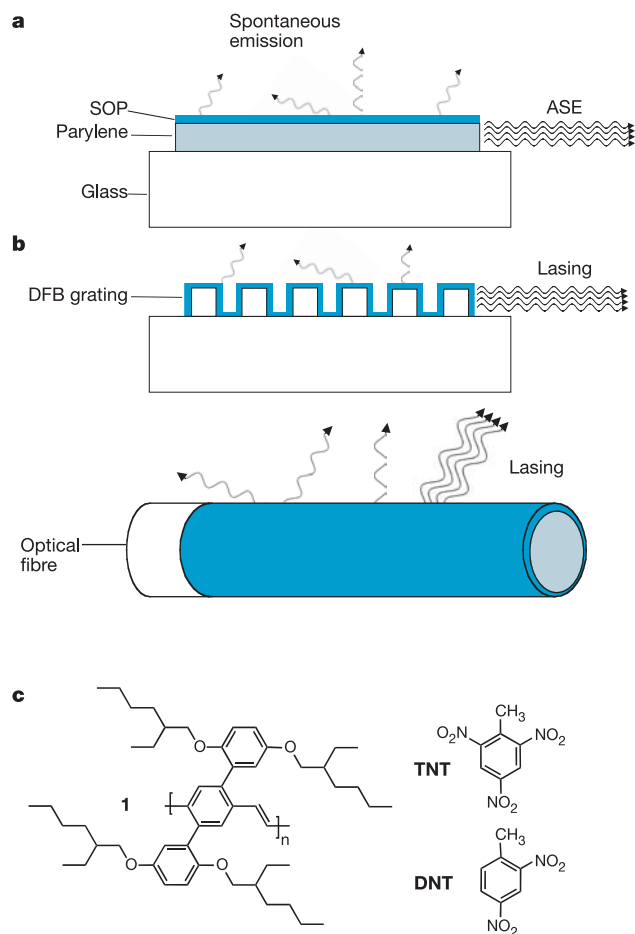
Figure 1 Test structures and materials used to demonstrate lasing chemosensory responses. **a**, Spin-coated polymer **1** films (40–80 nm thick, with refractive index $n = 1.70$) are coated on a transparent 200-nm-thick film of chemical vapour deposited parylene ($n = 1.67$), forming a two-layer index-matched waveguide on glass ($n = 1.45$). **b**, Spin-coated polymer **1** films (40 nm) coated on DFB gratings fabricated from polydimethylsiloxane. **c**, Ring-mode laser structure produced by dip coating polymer **1** on a 25 μm silica optical fibre. Inset, chemical structures of polymer **1**, TNT and DNT.
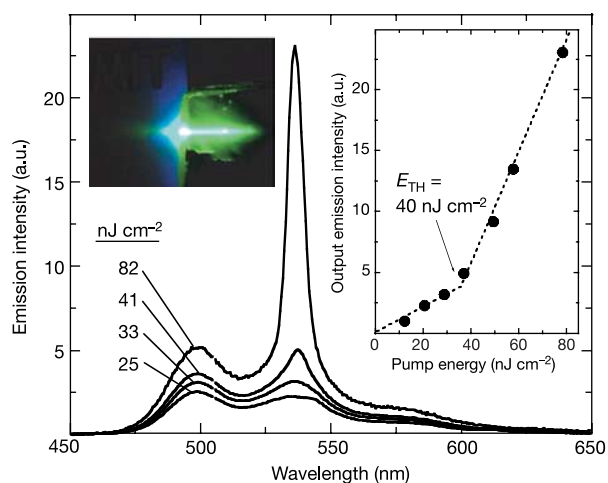
Figure 2 Stimulated and spontaneous emission of polymer **1** atop a polydimethylsiloxane DFB structure, which is shown in Fig. 1b. Main figure, emission spectra of polymer **1** structures at different pump energies show a low stimulated emission threshold (E_{TH}) of 40 nJ cm^{-2}. Right inset, emission intensity of the $\lambda = 535$ nm peak as a function of input power. Left inset, the polymer **1** film is pumped with a strip of $\lambda = 337$ nm pulsed light (right half of the photograph), resulting in a directional emission output (left) above threshold pump energies. a.u., arbitrary units.
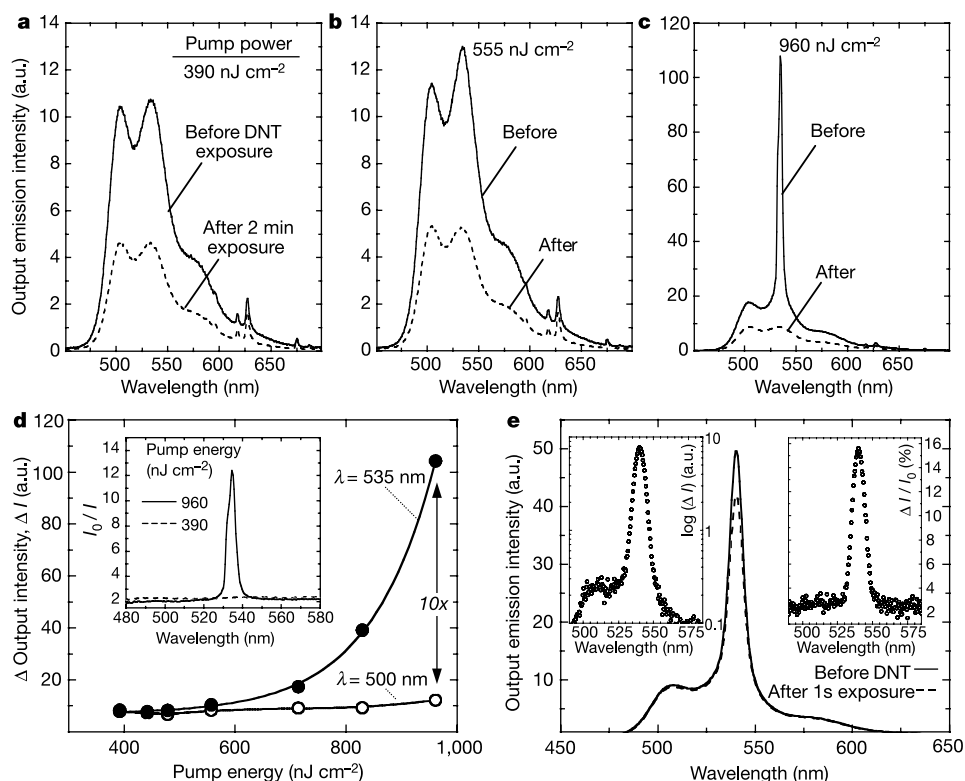
Figure 3 Performance of an optically pumped thin film of polymer **1** on parylene-coated glass before and after exposure to DNT. **a–c**, Spectral response of an optically pumped 80-nm-thick film of polymer **1** on parylene-coated glass (as in Fig. 1a) before and after a 2 min exposure to DNT. The nitrogen pump laser displays pulse-to-pulse power variations, and the approximate pulse energies E (in $\mathrm{nJ\,cm^{-2}}$) are: **a**, 390; **b**, 560; and **c**, 960. **d**, Change in the output emission intensity, I, at $\lambda = 500\,\mathrm{nm}$ (spontaneous emission; open circles) and $\lambda = 535\,\mathrm{nm}$ (ASE; filled circles) after 2 min DNT exposure as a function of input power. ASE differential caused by quenching shows an increase at higher powers. Inset, emission intensity before exposure to DNT, I_0, divided by emission intensity after the exposure, I, plotted for $E = 390$ and $960\,\mathrm{nJ\,cm^{-2}}$. The largest response occurs at ASE wavelengths ($\lambda = 535\,\mathrm{nm}$). **e**, Spectral response of a 40-nm-thick film of polymer **1** on parylene-coated glass before and after 1 s exposure to DNT, showing the sizable reduction in the ASE signal with almost no reduction in the spontaneous emission. Plots of the change in the output emission intensity I (left inset) and I/I_0 (right inset) show the sensitivity enhancement of 30-fold and fivefold, respectively. The measurement method will therefore determine the ultimate enhancement realized with lasing. The second case represents the minimum enhancement without additional signal processing (that is, averaging).

The ASE performance of polymer **1** compares favourably with previous best demonstrations of stimulated emission in organic materials. The ASE threshold of polymer **1** is significantly lower than the recently reported $E_{TH} = 3{,}200\,\mathrm{nJ\,cm^{-2}}$ (corresponding to a peak pump power of $P_{TH} = 3.2\,\mathrm{kW\,cm^{-2}}$) for polyfluorene lasers in a DFB structure[16] and the earlier record of $P_{TH} = 200\,\mathrm{W\,cm^{-2}}$ ($E_{TH} = 400\,\mathrm{nJ\,cm^{-2}}$) and $P_{TH} = 85\,\mathrm{W\,cm^{-2}}$ ($E_{TH} = 100\,\mathrm{nJ\,cm^{-2}}$) for doped polymer and doped molecular organic thin films, respectively[17]. The improved performance of polymer **1** structures is associated with the improved molecular design that maximizes the thin-film absorption and luminescence efficiency, maximizing the optical gain.
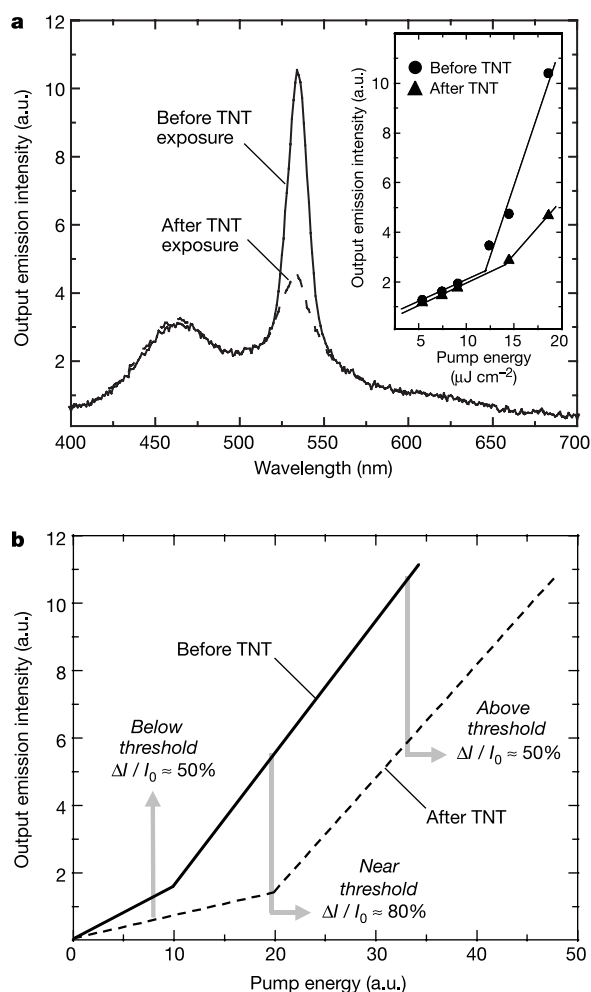
To validate the lasing enhanced sensing principle, we have made comparisons of the sensory responses of the spontaneous emission and ASE of **1** to a static saturated vapour pressure of DNT in air (Fig. 3). The differential sensitivity is readily apparent in a film before and after a 2-min exposure to DNT (Fig. 3a–c), wherein the spontaneous emission at $\lambda = 500\,\mathrm{nm}$ displays approximately a twofold quenching independent of laser power. However, at excitation levels above threshold power, $P_{TH} = 235\,\mathrm{W\,cm^{-2}}$ (corresponding to $E_{TH} = 960\,\mathrm{nJ\,cm^{-2}}$), the $\lambda = 535\,\mathrm{nm}$ ASE displays a tenfold drop in intensity (Fig. 3d). The differences are even more profound at lower quenching levels afforded by a one-second exposure time of films to saturated DNT vapour, in which we observed a significant attenuation in the ASE peak which is reproducibly >30-fold more sensitive than the attenuation in the spontaneous peak (Fig. 3e).

Whereas signal attenuation due to DNT was readily detected in these studies, measuring a similar response to TNT vapour proved more challenging. This analyte not only has a lower, easily depleted vapour pressure but also tends to bind tightly to the SOP surface and so is ineffective at quenching excitons generated more than 15 nm deep (the expected exciton diffusion length) in the films. This latter point prompted us to produce ring-mode lasing structures with a thin SOP film by dip-coating a 25-μm-diameter silica fibre with solution of **1** (10 mg per ml hexane). Attenuation in the lasing action on exposure to 5 p.p.b. TNT is observed again while the spontaneous emission of the system remains unchanged (Fig. 4a).

To understand better the origins of the enhanced sensitivity from lasing action, we have modelled the SOP as a standard four-level laser system. The four SOP lasing levels are, in order of increasing energy: (1) the electronic and geometric ground state of the SOP, (2) the electronic ground state and the nuclear excited state, (3) the electronic excited state and nuclear ground state, and (4) the electronic and nuclear excited state of the SOP. From this analysis (see Supplementary Information part B), it is evident that E_{TH} is increased in the presence of TNT and that the chemical sensitivity is determined by the excitation power. The specific considerations are illustrated in a plot of lasing threshold (Fig. 4b). Simple inspection shows that the optimal sensitivity (largest percentage reduction in signal) is obtained when the excitation power of the TNT-quenched polymer is at the onset of ASE. Hence, for ultra-trace detection, the pump power should be only slightly above the E_{TH} of the unquenched polymer.

It is also noteworthy that the difference in emission intensity before and after TNT exposure continues to increase as input power

3. McQuade, D. T., Pullen, A. E. & Swager, T. M. Conjugated polymer-based sensory materials. *Chem. Rev.* **100,** 2537–2574 (2000).
4. Tessler, N., Denton, G. J. & Friend, R. H. Lasing from conjugated-polymer microcavities. *Nature* **382,** 695–697 (1996).
5. Yang, J.-S. & Swager, T. M. Porous shape persistent fluorescent polymer films: An approach to TNT sensory materials. *J. Am. Chem. Soc.* **120,** 5321–5322 (1998).
6. Cumming, C. J. *et al.* Using novel fluorescent polymers as sensory materials for above-ground sensing of chemical signature compounds emanating from buried landmines. *IEEE Trans. Geosci. Remote Sens.* **39,** 1119–1128 (2001).
7. Rose, A., Lugmair, C. G. & Swager, T. M. Excited-state lifetime modulation in triphenylene-based conjugated polymers. *J. Am. Chem. Soc.* **123,** 11298–11299 (2001).
8. Zahn, S. & Swager, T. M. Three-dimensional electronic delocalization in chiral conjugated polymers. *Angew. Chem. Int. Edn Engl.* **41,** 4225–4230 (2002).
9. Kozlov, V. G., Bulović, V., Burrows, P. E. & Forrest, S. F. Laser action in organic semiconductor waveguide and double heterostructure devices. *Nature* **389,** 362–365 (1997).
10. Bulović, V., Kozlov, V. G., Khalfin, V. B. & Forrest, S. R. Transform-limited, narrow-linewidth lasing action in organic semiconductor microcavities. *Science* **279,** 553–555 (1998).
11. Scherf, U., Riechel, S., Lemmer, U. & Mahrt, R. F. Conjugated polymers: lasing and stimulated emission. *Curr. Opin. Solid State Mater. Sci.* **5,** 143–154 (2001).
12. Halls, J. J. M., Pichler, K., Friend, R. H., Moratti, S. C. & Holmes, A. B. Exciton diffusion and dissociation in a poly(*p*-phenylenevinylene)/C₆₀ heterojunction photovoltaic cell. *Appl. Phys. Lett.* **68,** 3120–3122 (1996).
13. Hamer, P. J. *et al.* Optical studies of chemical doping achieved by ion implantation in poly(p-phenylene vinylene). *Phil. Mag. B* **73,** 367–382 (1996).
14. Levitsky, I. A., Kim, J. & Swager, T. M. Energy migration in a poly(phenylene ethynylene): determination of interpolymer transport in anisotropic Langmuir-Blodgett films. *J. Am. Chem. Soc.* **121,** 1466–1472 (1999).
15. Kogelnik, H. & Shank, C. V. Stimulated emission in a periodic structure. *Appl. Phys. Lett.* **18,** 152–154 (1971).
16. Heliotis, G. *et al.* Emission characteristics and performance comparison of polyfluorene lasers with one- and two-dimensional distributed feedback. *Adv. Funct. Mater.* **14,** 91–97 (2004).
17. Berggren, M., Dodabalapur, A., Slusher, R. E. & Bao, Z. Light amplification in organic thin films using cascade energy transfer. *Nature* **389,** 466–469 (1997).
18. Yang, Y.-S. & Swager, T. M. Fluorescent porous polymer films as TNT chemosensors: electronic and structural effects. *J. Am. Chem. Soc.* **120,** 11864–11873 (1998).

Figure 4 Response of a ring-mode laser coated with polymer **1**. **a**, Spectral response of a ring-mode structure consisting of a 25-μm diameter silica fibre dip-coated with a polymer **1** thin film. ASE attenuation in the absence of spontaneous emission attenuation after 1.5 min exposure to saturated TNT vapour pressure. Inset, plots of ASE peak emission intensity (λ = 535 nm) as a function of excitation power. TNT exposure increases the pump energy threshold. **b**, A general sketch of the ASE E_{TH} increase after exposure of the SOP film to a quencher such as TNT. The change in the output emission intensity divided by the initial output emission intensity, I/I_0, is largest at pump energies just below the E_{TH} of analyte-exposed films.

increases, which results in a quenching signal of larger magnitude. Unfortunately, with longer operating times (>1 min), the higher excitation power can lead to photobleaching, which interferes with the quenching response. Nevertheless, in instances where the greatest amount of signal is required, one may achieve this through increasing the excitation power, which shortens the operating lifetime of the active polymer film.

The strong binding of the nitroaromatic analytes DNT and TNT to electron-rich SOPs and their ease of reduction makes for a selective response that is relatively immune to interference[6,18], and no response was observed upon exposure of our devices to benzene or naphthalene. Current and future efforts focus on incorporating SOPs into high-*Q* optical feedback structures that will allow further reduction in E_{TH} as well as an enhanced sensitivity with reduced thickness of the active layer.   □

1. Zhou, Q. & Swager, T. M. Methodology for enhancing the sensitivity of fluorescent chemosensors: energy migration in conjugated polymers. *J. Am. Chem. Soc.* **117,** 7017–7018 (1995).
2. Swager, T. M. The molecular wire approach to sensory signal amplification. *Acc. Chem. Res.* **31,** 201–207 (1998).

Light-induced shape-memory polymers

Andreas Lendlein[1,2], Hongyan Jiang[2,3], Oliver Jünger[2]* & Robert Langer[4]

[1]*GKSS Research Center Geesthacht GmbH, Institute of Chemistry, Kantstraβe 55, D-14513 Teltow, Germany*
[2]*Institute for Technology and Development of Medical Devices, RWTH Aachen, Pauwelsstraβe 30, and* [3]*mnemoScience GmbH, Pauwelsstraβe 19, D-52074 Aachen, Germany*
[4]*Department of Chemical Engineering, Massachusetts Institute of Technology, 45 Carleton Street, Cambridge, Massachusetts 02139, USA*

* Present address: Prof.-Staudinger-Strasse, D-65451 Kelsterbach, Germany

Materials are said to show a shape-memory effect if they can be deformed and fixed into a temporary shape, and recover their original, permanent shape only on exposure to an external stimulus[1–3]. Shape-memory polymers have received increasing attention because of their scientific and technological significance[4,5]. In principle, a thermally induced shape-memory effect can be activated by an increase in temperature (also obtained by heating on exposure to an electrical current[6] or light illumination[6,7]). Several papers have described light-induced changes in